Roles of the DOCK-D family proteins in a mouse model of neuroinflammation

Received for publication, August 1, 2019, and in revised form, March 16, 2020 Published, Papers in Press, April 2, 2020, DOI 10.1074/jbc.RA119.010438

Kazuhiko Namekata, Xiaoli Guo, Atsuko Kimura, Yuriko Azuchi, Yuta Kitamura, Chikako Harada, and Takayuki Harada[1]

From the Visual Research Project, Tokyo Metropolitan Institute of Medical Science, Tokyo 156-8506, Japan

Edited by Paul E. Fraser

The DOCK-D (dedicator of cytokinesis D) family proteins are atypical guanine nucleotide exchange factors that regulate Rho GTPase activity. The family consists of Zizimin1 (DOCK9), Zizimin2 (DOCK11), and Zizimin3 (DOCK10). Functions of the DOCK-D family proteins are presently not well-explored, and the role of the DOCK-D family in neuroinflammation is unknown. In this study, we generated three mouse lines in which *DOCK9* (*DOCK9*$^{-/-}$), *DOCK10* (*DOCK10*$^{-/-}$), or *DOCK11* (*DOCK11*$^{-/-}$) had been deleted and examined the phenotypic effects of these gene deletions in MOG$_{35-55}$ peptide-induced experimental autoimmune encephalomyelitis, an animal model of the neuroinflammatory disorder multiple sclerosis. We found that all the gene knockout lines were healthy and viable. The only phenotype observed under normal conditions was a slightly smaller proportion of B cells in splenocytes in *DOCK10*$^{-/-}$ mice than in the other mouse lines. We also found that the migration ability of macrophages is impaired in *DOCK10*$^{-/-}$ and *DOCK11*$^{-/-}$ mice and that the severity of experimental autoimmune encephalomyelitis was ameliorated only in *DOCK10*$^{-/-}$ mice. No apparent phenotype was observed for *DOCK9*$^{-/-}$ mice. Further investigations indicated that lipopolysaccharide stimulation up-regulates *DOCK10* expression in microglia and that microglial migration is decreased in *DOCK10*$^{-/-}$ mice. Up-regulation of C–C motif chemokine ligand 2 (CCL2) expression induced by activation of Toll-like receptor 4 or 9 signaling was reduced in *DOCK10*$^{-/-}$ astrocytes compared with WT astrocytes. Taken together, our findings suggest that DOCK10 plays a role in innate immunity and neuroinflammation and might represent a potential therapeutic target for managing multiple sclerosis.

The dedicator of cytokinesis (DOCK) proteins are atypical guanine nucleotide exchange factors (GEFs)[2] that regulate Rho GTPase activity. To date, 11 members (DOCK1–11) have been identified, and they are divided into four families: DOCK-A (DOCK1, DOCK2, and DOCK5), DOCK-B (DOCK3 and DOCK4), DOCK-C (DOCK6, DOCK7, and DOCK8), and DOCK-D (Zizimin1 (DOCK9), Zizimin3 (DOCK10), and Zizimin2 (DOCK11)) (1–3). The DOCK proteins in the same family share similar sequence homology, and although DOCK-A, DOCK-B and DOCK-C families are relatively well-studied, the information on the function of the DOCK-D family is very limited. The DOCK-D family proteins all activate the Rho GTPase Cdc42, with DOCK10 also activating Rac1 (4), and they all possess N-terminal PH domains, without the SH3 domain or the proline-rich region that are common features for DOCK-A and DOCK-B.

DOCK9 mutations are found in patients with keratoconus (5), an eye disease with progressive thinning of the cornea leading to visual impairment, and it contributes to invasive activity of glioblastoma cells (6). It has also been reported that DOCK9 interacts with DOCK4 and promotes remodeling of lateral organization of endothelial cells and lumen morphogenesis (7). It is highly expressed in the brain (8); interestingly, DOCK9 has been identified as a novel interactor of α-amino-3-hydroxy-5-methyl-4-isoxazolepropionic acid receptors in the brain (9) and regulates neuronal trafficking of these receptors, suggesting its role in synaptic plasticity (10). Overexpression of DOCK9 promotes dendrite growth in the hippocampus (11), indicating that it plays an important role in the central nervous system (CNS).

DOCK10 is expressed in the brain, spleen, and thymus (8), suggesting that it may play a role in neuroinflammation. DOCK10 is up-regulated in B cells by stimulation with interleukin-4, an effect that is not observed with DOCK9 or DOCK11 (12). Studies with *DOCK10*$^{-/-}$ mice showed that DOCK10 plays a role in B-cell maturation and function (13, 14). However, mice with B cell–specific deletion of DOCK10 showed normal development and mild decline in B-cell activation (15), suggesting that the role of DOCK10 in B cells may be small. Recent studies based on transcriptome analyses demonstrated that *DOCK10*$^{-/-}$ mice live longer than WT mice (16), indicating that DOCK10 is involved in aging processes.

DOCK11 is highly expressed in the spleen and thymus, suggesting its role in the immune system (8). Not very much information is available at present, but deficiency in DOCK11 causes

This work was supported in part by Japan Society for the Promotion of Science KAKENHI Grants-in-Aid for Scientific Research JP20K07751 (to K. N.), JP17K07123 and JP20K09820 (to A. K.), JP20K18404 (to Y. K.), JP19K09943 (to C. H.), and JP18K19625 (to T. H.) and funds from the Taiju Life Social Welfare Foundation (to T. H.) and the Takeda Science Foundation (to T. H.). The authors declare that they have no conflicts of interest with the contents of this article.

This article contains Figs. S1–S3.

[1] To whom correspondence should be addressed: Visual Research Project, Tokyo Metropolitan Institute of Medical Science, 2-1-6 Kamikitazawa, Setagaya-ku, Tokyo 156-8506, Japan. Tel.: 81-3-6834-2338; Fax: 81-3-5316-3150; E-mail: harada-tk@igakuken.or.jp.

[2] The abbreviations used are: GEF, guanine nucleotide exchange factor; EAE, experimental autoimmune encephalomyelitis; MS, multiple sclerosis; TLR, Toll-like receptor; CNS, central nervous system; MBP, myelin basic protein; mfERG, multifocal electroretinogram; MOG, myelin oligodendrocyte glycoprotein; LPS, lipopolysaccharide; CFSE, carboxyfluorescein diacetate succinimidyl ester; BMDM, bone marrow-derived macrophage; qPCR, quantitative PCR.

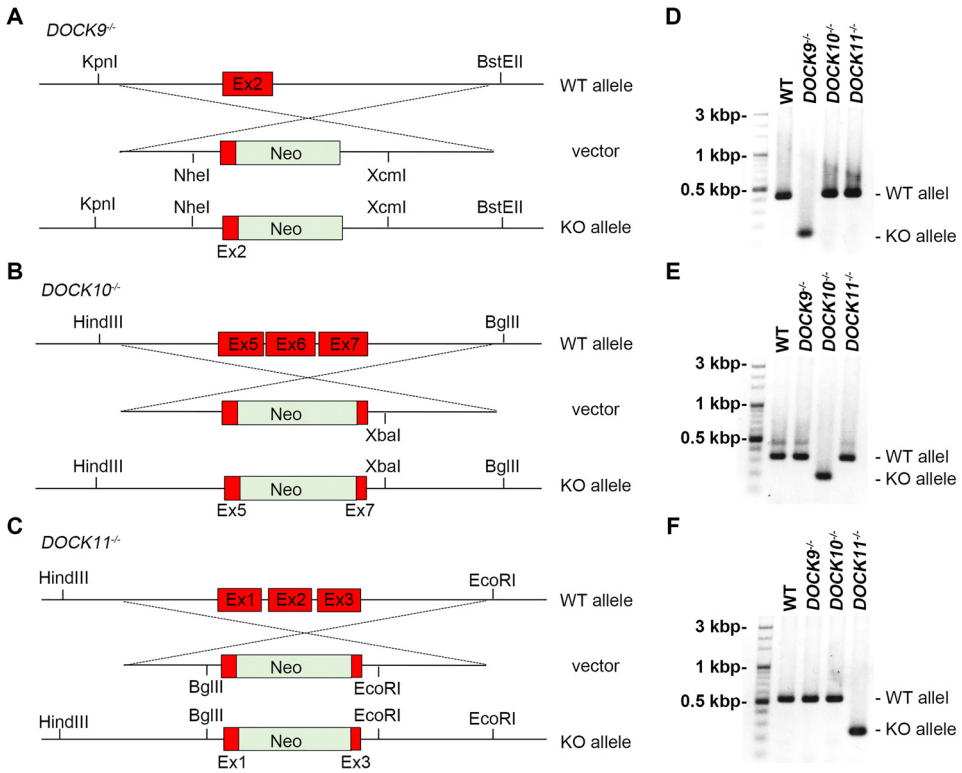

Figure 1. Generation of the DOCK-D family gene knockout mice. *A–C*, targeting vectors used to generate *DOCK9*$^{-/-}$ (*A*), *DOCK10*$^{-/-}$ (*B*), and *DOCK11*$^{-/-}$ (*C*) mice. *D–F*, examples of genotyping using tail DNA from WT, *DOCK9*$^{-/-}$, *DOCK10*$^{-/-}$, and *DOCK11*$^{-/-}$ mice with primer sets for *DOCK9* (*D*), *DOCK10* (*E*), and *DOCK11* (*F*).

abnormalities in B cells (14), and expression of DOCK11, but not DOCK9, is decreased in aged mice (17, 18), suggesting a role of DOCK11 in aging. Taken together, the tissue distribution of DOCK9, DOCK10, and DOCK11 and their functional features, though information is limited, indicated the possibility that these proteins play a role in immune disorders; however, whether any of the DOCK-D family proteins play a role in neuroinflammation or not is unknown.

Multiple sclerosis (MS) is a progressive neuroinflammatory demyelinating disease of the CNS. Experimental autoimmune encephalomyelitis (EAE) is a classical model that shares clinical and pathological characteristics with MS. It is widely used to study pathogenesis of MS and explore therapeutic targets (19, 20). There is vast evidence of a role of the adaptive immunity in pathogenesis of MS and EAE, but innate immunity, involving microglia/macrophages and astrocytes, also plays an important role in both triggering and amplifying neuroinflammation (21–23). The Rho GTPases regulate important functional responses in innate immunity via actin dynamics, and Cdc42 is a key regulator of astrocytic cell polarity and migration following injury (24, 25). In this study, we generated three novel mouse lines with deletion in DOCK9, DOCK10, or DOCK11, and examined the role of the DOCK-D family proteins in neuroinflammation using a mouse model of MS.

Results

Deficiency in the DOCK-D family member has no or little effect on the development of neural and immune cells

To elucidate the functions of DOCK-D family members in detail, we generated the DOCK-D family knockout mice, namely DOCK9-deficient (*DOCK9*$^{-/-}$), DOCK10-deficient (*DOCK10*$^{-/-}$), and DOCK11-deficient (*DOCK11*$^{-/-}$) mice (Fig. 1, *A–C*). Examples of genotyping for each knockout mouse line, using tail DNA, are also shown (Fig. 1, *D–F*). We first investigated the effects of the deficiency in the DOCK-D family member on the development of the CNS and immune system.

To this aim, we first examined the retina, optic nerve and spinal cord to determine whether neural cells and myelin are affected by the lack of the DOCK-D family. Retinal cross-sections of adult WT, *DOCK9*$^{-/-}$, *DOCK10*$^{-/-}$, and *DOCK11*$^{-/-}$ mice were stained with an anti-GLAST antibody for Müller glial cells and an anti-NeuN antibody for detection of retinal ganglion cells (*top row* in Fig. 2*A*). Both kinds of staining showed no difference among the mouse lines. Moreover, myelin basic protein (MBP) or MBP/NeuN staining of the optic nerves or spinal cord sections, respectively, also revealed no difference among the mice (*middle* and *bottom rows* in Fig. 2*A*). We also examined the expression of astrocytes, microglia, neurons, and myelin in the spinal cord at P10 but found no abnormalities in *DOCK9*$^{-/-}$, *DOCK10*$^{-/-}$, and *DOCK11*$^{-/-}$ mice (Fig. S1), indicating that development of neural cells and myelin was not affected by DOCK-D deficiency. We also examined whether there was any deficit in nervous function in these mice. For this, we assessed visual function by multifocal electroretinogram (mfERG) and motor performance by a rotarod test. We found no impairment in visual function or motor performance by the lack of DOCK-D family proteins (Fig. 2, *B–E*). We next investigated the effects of the deficiency in the DOCK-D family member on the development of the immune system. FACS analysis of the splenocytes revealed no difference in the popu-

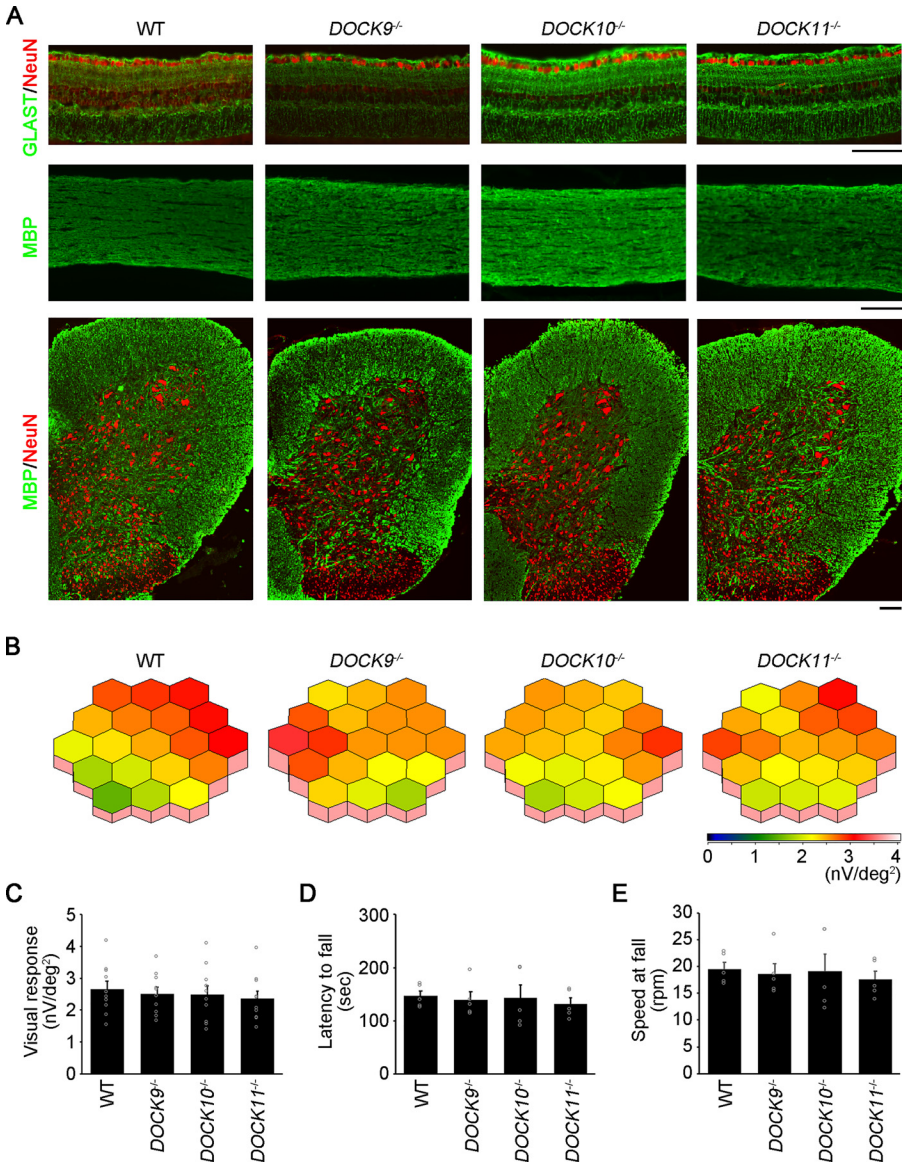

Figure 2. Effects of the deficiency in the DOCK-D family members on the development of the central nervous system. *Top row*, GLAST/NeuN double immunostaining of the retina of WT, *DOCK9*$^{-/-}$, *DOCK10*$^{-/-}$, and *DOCK11*$^{-/-}$ mice. *Middle row*, MBP staining of the optic nerves of WT, *DOCK9*$^{-/-}$, *DOCK10*$^{-/-}$, and *DOCK11*$^{-/-}$ mice. *Bottom row*, MBP/NeuN double immunostaining of the spinal cords of WT, *DOCK9*$^{-/-}$, *DOCK10*$^{-/-}$, and *DOCK11*$^{-/-}$ mice. *Scale bars*, 100 μm. *B*, representative images of three-dimensional plots showing averaged visual responses examined by mfERG in WT, *DOCK9*$^{-/-}$, *DOCK10*$^{-/-}$, and *DOCK11*$^{-/-}$ mice. The degree of retinal responses is presented in the *color bar*. A higher score (*red*) indicates highly sensitive visual responses, and a lower score (*green*) indicates impaired retinal responses. *C*, quantitative analysis of *B*. The data are presented as mean values, and the *error bars* represent S.E. ($n = 10$ eyes). *D*, latency to fall in the accelerated rotarod test in WT, *DOCK9*$^{-/-}$, *DOCK10*$^{-/-}$, and *DOCK11*$^{-/-}$ mice. The data are presented as mean values, and the *error bars* represent S.E. ($n = 5$). *E*, speed at fall in the accelerated rotarod test in WT, *DOCK9*$^{-/-}$, *DOCK10*$^{-/-}$, and *DOCK11*$^{-/-}$ mice. The data are presented as mean values, and the *error bars* represent S.E. ($n = 5$).

lation of $CD3^+CD4^+$ T cells, $CD3^+CD8^+$ T cells, and $CD11C^+$ dendritic cells among the mice (Fig. 3, *A–C*), whereas a mild reduction in the population of $B220^+$ B cells was found in *DOCK10*$^{-/-}$ mice compared with WT mice (Fig. 3*D*). Taken together, these results demonstrated that the DOCK-D family has no or little effects on the development of the CNS and immune system.

Because DOCK-D family members are GEFs that are involved in actin cytoskeleton dynamics, we investigated the effects of the deficiency in the DOCK-D family on T-cell proliferation and macrophage migration, both of which require GEF-mediated actin polymerization. The *in vitro* proliferation assay showed no difference in T cell proliferation with DOCK-D family member deficiency (Fig. 4*A*). We then investigated the effects of the deficiency in the DOCK-D family member on macrophage migration by using a Boyden chamber assay. We measured the chemotactic response of macrophage migration from the control medium (top chamber) toward medium containing 50 ng/ml of C–C motif chemokine ligand 2 (CCL2; bottom chamber). Interestingly, CCL2-induced cell migration activity was reduced significantly in *DOCK10*- or *DOCK11*-deficient macrophages (Fig. 4, *B* and *C*), indicating that GEF activity of DOCK10 and DOCK11 was involved in macrophage migration. These results suggest that the DOCK-D family, mainly DOCK10 and DOCK11, may play a role in some diseases in which macrophages are involved.

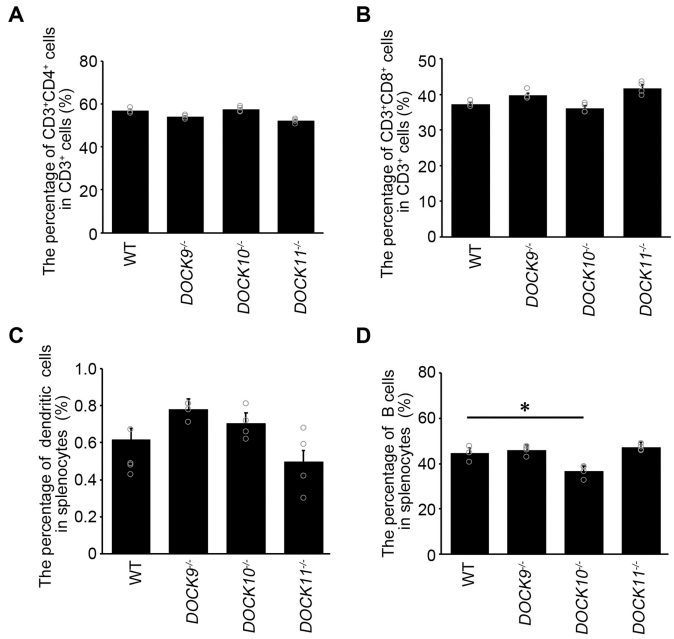

Figure 3. Effects on the development of immune cells in the absence of DOCK-D family member proteins. The percentages of $CD3^+CD4^+$ T cells (*A*), $CD3^+CD8^+$ T cells (*B*), $CD11C^+$ dendritic cells (*C*), and $B220^+$ B cells (*D*) in $CD3^+$ cells (*A* and *B*) and in splenocytes (*C* and *D*) are shown. The cells were isolated from WT, *DOCK9*$^{-/-}$, *DOCK10*$^{-/-}$, and *DOCK11*$^{-/-}$ mice and analyzed by FACS. The data are presented as mean values, and the *error bars* represent S.E. ($n = 4$). *, $p < 0.01$, Dunnett's test for multiple comparisons to WT.

Impaired microglia/astrocyte activation with DOCK10, but not DOCK9 or DOCK11 deficiency

We then investigated the effects of the deficiency in the DOCK-D family member on myelin oligodendrocyte glycoprotein (MOG)–induced EAE, a disease model in which macrophages play an important role in pathogenesis of disease progression. The disease severity of *DOCK10*$^{-/-}$ EAE mice, as demonstrated by clinical scores, was significantly reduced after day 16 compared with WT EAE mice (Fig. 5*A*). However, EAE severities of *DOCK9*$^{-/-}$ and *DOCK11*$^{-/-}$ mice remained comparable with those of WT mice (Fig. 5*A*). Pathological analysis of the spinal cords revealed a large amount of infiltrating cells and demyelination in WT, *DOCK9*$^{-/-}$, and *DOCK11*$^{-/-}$ EAE mice, which were reduced in *DOCK10*$^{-/-}$ EAE mice (Fig. 5, *B* and *D*). A similar trend of reduction in infiltrating cells and demyelination was found in the optic nerves of *DOCK10*$^{-/-}$ EAE mice (Fig. 5, *C* and *E*). We further analyzed EAE pathology in WT and *DOCK10*$^{-/-}$ mice (Fig. 6). We examined the expressions of CD3, B220, iba1, and GFAP in the spinal cord and optic nerve of WT and *DOCK10*$^{-/-}$ mice at days 0, 12, and 30 after MOG administration. There was a large increase in the number of CD3+ cells, B220+ cells, iba1+ cells, and GFAP+ cells at day 12 in the spinal cord of both WT and *DOCK10*$^{-/-}$ mice, with no significant difference between them, but at day 30, the numbers of all these four types of cells were significantly lower in *DOCK10*$^{-/-}$ mice compared with WT mice (Fig. 6, *A* and *B*). Similar trends were observed in the optic nerve (Fig. 6, *C* and *D*). In addition, EAE caused weight loss in WT mice by day 30, but this was not observed in *DOCK10*$^{-/-}$ mice (Fig. S2). We next investigated possible mechanisms contributing to the different effects of the DOCK-D family members on EAE.

It has been reported that expression of *DOCK9* and *DOCK10*, but not *DOCK11*, were detected in the brain by Northern blotting analysis (8). To find out which cell types in the CNS show high expression of these genes, we assessed their expressions using primary cultured neurons, astrocytes, and microglial cells. Quantitative PCR analysis revealed that *DOCK9* mRNA was expressed predominantly in neurons and relatively low expression of *DOCK11* mRNA in astrocytes compared with neurons or astrocytes (Fig. 7*A*). On the other hand, we detected a significantly high expression of *DOCK10* mRNA in microglia compared with neurons or astrocytes (Fig. 7*A*).

DOCK10 is known to be induced by interleukin-4 in chronic lymphocytic leukemia cells and in human peripheral blood B lymphocytes but not T lymphocytes (12, 15, 26). We investigated whether DOCK-D family gene expressions could be up-regulated by an inflammatory stimulus in microglial cells, the primary immune cells of the CNS. The expression of *DOCK10* was significantly up-regulated in microglial cells stimulated with lipopolysaccharide (LPS), whereas expressions of *DOCK9* or *DOCK11* were unchanged (Fig. 7*B*). Taken together, these results indicate that *DOCK10* deficiency might have effects on the function of microglia.

We then investigated the effects of *DOCK10* deficiency on microglial migration by using a Boyden chamber assay. We measured the chemotactic response of microglial migration from the control medium (top chamber) toward 50 μM ATP (bottom chamber). ATP induced migration of WT microglial cells, which was reduced significantly by *DOCK10* deficiency (Fig. 7, *C* and *D*), indicating that microglial migration was impaired by *DOCK10* deficiency.

We found that *DOCK10* mRNA expression in astrocytes was relatively high, unlike *DOCK9* or *DOCK11* (Fig. 7*A*). Therefore, we next investigated the effects of *DOCK10* deficiency on astrocytic activity by measuring Toll-like receptor (TLR) 4- or TLR9-mediated CCL2 production from astrocytes, which has an important role during neuroinflammation. CCL2 production, as measured by ELISA, was up-regulated in WT astrocytes stimulated with LPS or CpG, which was significantly reduced in astrocytes with *DOCK10* deficiency (Fig. 7*E*). Together, these results indicate that activities of not only microglia but also astrocytes were impaired by *DOCK10* deficiency, which might partially contribute to the ameliorated severity in *DOCK10*$^{-/-}$ EAE mice.

Discussion

In this study, we examined the role of the DOCK-D family members in the CNS by generating and studying the knockout mice. To our knowledge, this is the first study to report *DOCK9*$^{-/-}$ mice. We found that deletion of the DOCK-D family member genes in mice did not cause severe developmental abnormalities, but the proportion of B cells in splenocytes in *DOCK10*$^{-/-}$ mice was smaller than WT mice, and the migration ability of macrophages is decreased in *DOCK10*$^{-/-}$ and *DOCK11*$^{-/-}$ mice. We investigated the roles of the DOCK-D family members in EAE, and the disease severity was reduced in *DOCK10*$^{-/-}$ mice, but not in *DOCK9*$^{-/-}$ or *DOCK11*$^{-/-}$

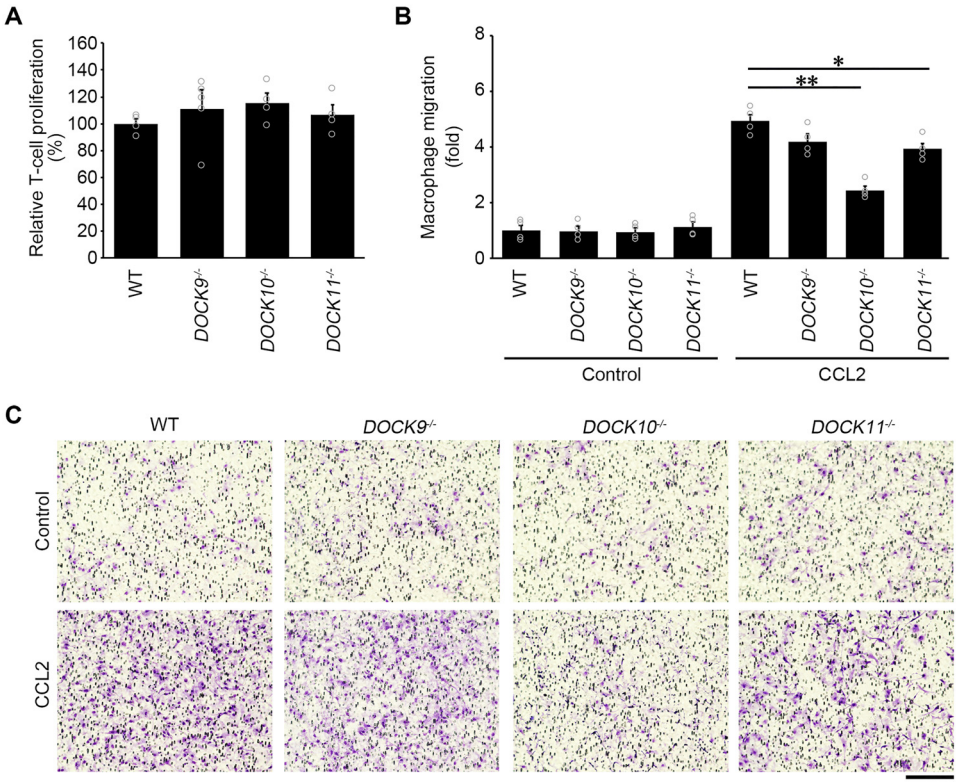

Figure 4. Effects of the deficiency in the DOCK-D family members on T-cell proliferation and macrophage migration. *A*, quantification of anti-CD3 T-cell proliferation analyzed by FACS. Splenocytes isolated from WT, *DOCK9*$^{-/-}$, *DOCK10*$^{-/-}$, and *DOCK11*$^{-/-}$ mice were used. *B*, quantification analysis of CCL2-dependent migration by BMDM. *C*, migration ability of BMDM was examined using a Boyden chamber assay. The data are presented as mean values, and the *error bars* represent S.E. ($n = 4$). *, $p < 0.05$; **, $p < 0.01$, Dunnett's test for multiple comparisons to WT between CCL2-stimulated groups. *Scale bar*, 100 μm.

mice. We revealed that LPS stimulation induces up-regulation of DOCK10 in microglia, and the migration ability of microglia is decreased in *DOCK10*$^{-/-}$ mice. In addition, CCL2 up-regulation in astrocytes by inflammatory stimuli was suppressed in *DOCK10*$^{-/-}$ astrocytes. These findings suggest that, among the DOCK-D family members, only DOCK10 plays a major role in neuroinflammation.

The role of the DOCK GEFs in neuroinflammation has been demonstrated previously. Studies have reported that a lack of DOCK8, which belongs to the DOCK-C family, leads to impaired activity of T cells and microglia, resulting in reduced EAE severity (27, 28). In this study, we demonstrated that a lack of DOCK10 does not affect T cells and dendritic cells, but it affects migration ability of macrophages and microglia. Macrophages and microglia play important roles in pathogenesis of EAE (29), and thus this may explain partly for the reduced EAE severity in *DOCK10*$^{-/-}$ mice. We also showed that LPS- or CpG-induced CCL2 up-regulation in astrocytes is reduced in *DOCK10*$^{-/-}$ mice. CCL2 produced by astrocytes are required for recruitment of macrophages and promotes EAE disease progression (30). We have previously reported that deletion of ASK1 (apoptosis signal–regulating kinase 1), a mitogen-activated protein kinase kinase kinase, ameliorates EAE disease severity by suppressing CCL2 up-regulation in astrocytes (31). Taken together, DOCK10 may contribute to the pathogenesis of EAE by regulating activities of macrophages, microglia, and astrocytes.

Little is known about the function of DOCK11 at present. One study with *DOCK11*$^{-/-}$ mice demonstrated that DOCK11 is involved in B-cell development, but not in immune responses (14). In this study, we show that the percentage of B cells in splenocytes is not affected, but the migration ability of macrophages is impaired in *DOCK11*$^{-/-}$ mice. Expression of microglial DOCK11 is not altered by LPS stimulation, and the apparent phenotype is absent in *DOCK11*$^{-/-}$ EAE mice. These findings suggest that although the effects may be small, DOCK11 plays a role in the activities of macrophages.

It was surprising to find the lack of phenotype in *DOCK9*$^{-/-}$ mice. Previous studies reported that DOCK9 is strongly expressed in the developing brain and that DOCK9 promotes dendrite outgrowth in hippocampal neurons (11). It is possible that there is a synaptic impairment that was not detected in our experimental paradigm. Further studies may include behavioral studies to test cognitive functions.

We were also surprised to find a distinctive phenotype only in *DOCK10*$^{-/-}$ mice, given the similarity in the structures among the DOCK-D family proteins. However, the distributions of these proteins differ in that DOCK9 is mainly expressed in the CNS and DOCK11 is mainly expressed in the immune system, whereas DOCK10 is expressed both in the CNS and immune system (8). In addition, whereas DOCK9 and DOCK11 are Cdc42 GEFs, DOCK10 is a GEF for both Cdc42 and Rac1 (4). Furthermore, we demonstrated that LPS stimulation up-regulates DOCK10, but not DOCK9 or DOCK11, in microglia,

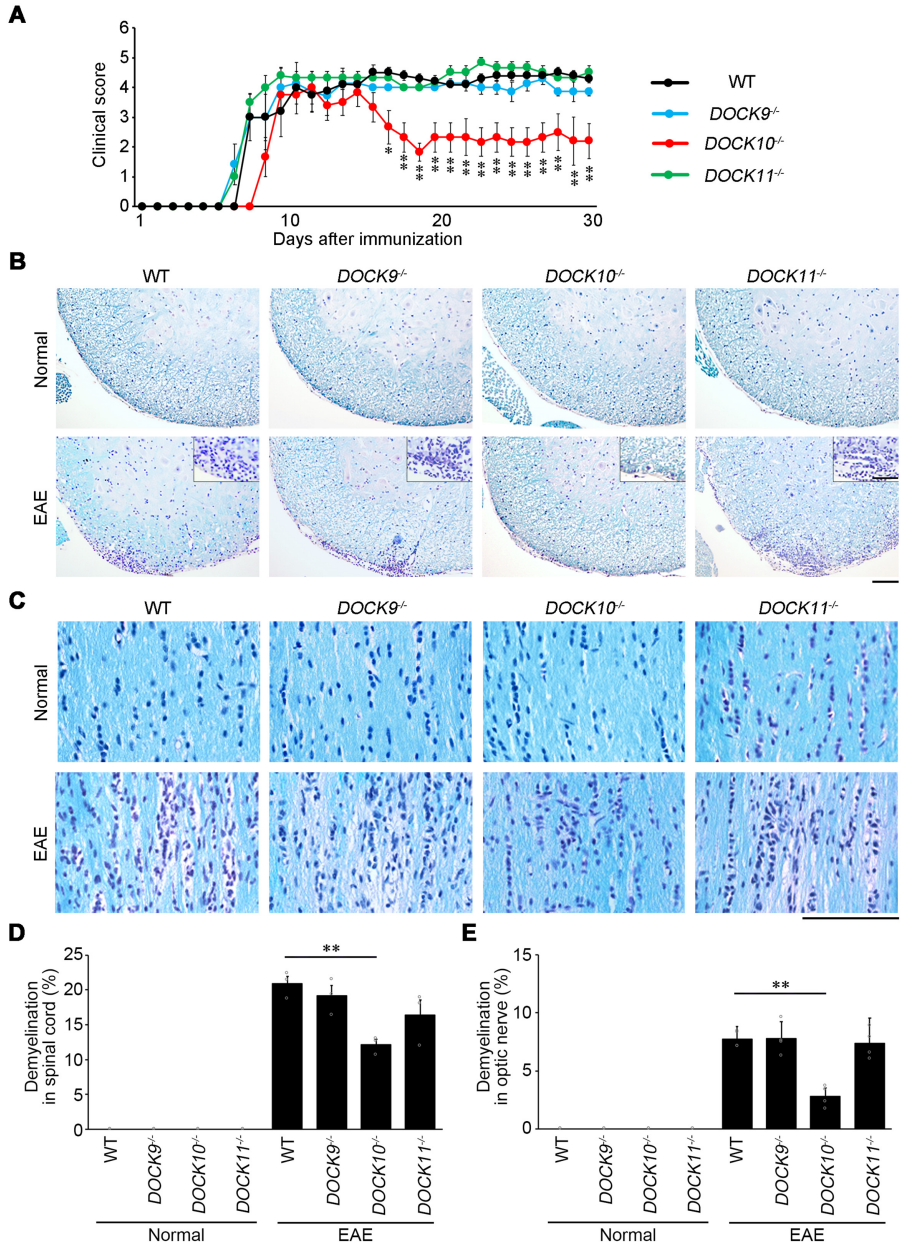

Figure 5. EAE severity was ameliorated in *DOCK10*$^{-/-}$ mice. *A*, clinical scores of WT, *DOCK9*$^{-/-}$, *DOCK10*$^{-/-}$, and *DOCK11*$^{-/-}$ EAE mice ($n = 11$ for WT; $n = 7$ for *DOCK9*$^{-/-}$; $n = 6$ for *DOCK10*$^{-/-}$; and $n = 6$ for *DOCK11*$^{-/-}$). The severity of EAE symptoms is reduced in *DOCK10*$^{-/-}$ EAE mice. *, $p < 0.05$; **, $p < 0.01$, Dunnett's test for multiple comparisons to WT. *B* and *C*, Luxol fast blue and hematoxylin–eosin staining of the spinal cords (*B*) and the optic nerves (*C*) of WT, *DOCK9*$^{-/-}$, *DOCK10*$^{-/-}$, and *DOCK11*$^{-/-}$ EAE mice at day 30. *Insets* in *B* show magnified (2×) regions of demyelination. *Scale bars* indicate 100 μm in *B*, 50 μm *insets* in *B*, and 100 μm in *C*. *D*, quantitative analysis of *B*. *E*, quantitative analysis of *C*. The data are presented as mean values, and the *error bars* represent S.E. ($n = 3$ for the spinal cord; and $n = 4$ for the optic nerve). *, $p < 0.05$; **, $p < 0.01$, Dunnett's test for multiple comparisons to WT.

suggesting that DOCK10 plays a role in microglia during inflammation. These differences must have caused the reduced severity of EAE only in *DOCK10*$^{-/-}$ mice, and future studies need to include cell type–specific deletion of DOCK10 in microglia or astrocytes to further elucidate the role of DOCK10 in neuroinflammation.

We demonstrated that TLR ligand-induced production of CCL2 by DOCK10$^{-/-}$ astrocytes was significantly smaller than WT astrocytes (Fig. 7*E*). However, it is important to note that microglia also produces CCL2 upon inflammatory stimulation; for example, in response to LPS stimulation, microglia may produce 1–5 times more CCL2 than astrocytes (32, 33). For this reason, we checked the purity of our astrocyte culture for microglial contamination using immunohistochemistry. We found that although many GFAP-positive cells are detected, the number of Iba1-positive cells is very small (Fig. S3). Therefore, one may assume that contribution of microglia in our setup is small, although we cannot discard the possibility that the observed effects are partly due to microglia.

In summary, we report that DOCK9 and DOCK11 have little or no effect on the pathogenesis of EAE. However, the disease severity of EAE was ameliorated in *DOCK10*$^{-/-}$ mice, suggesting differential biological roles of the DOCK-D family proteins

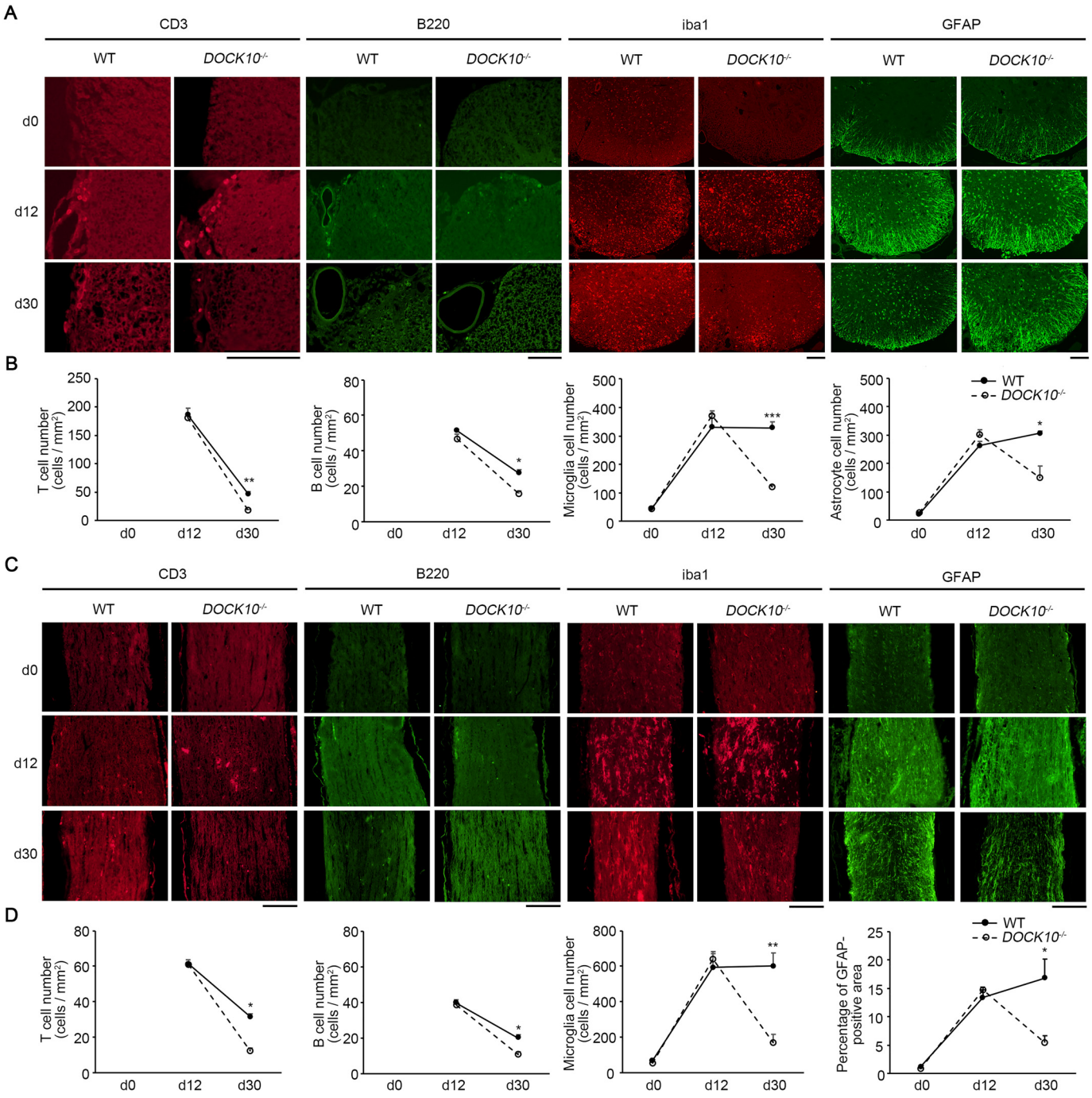

Figure 6. Infiltration of T cells, B cells, microglia, and astrocytes are reduced in *DOCK10*$^{-/-}$ EAE mice. *A* and *B*, immunostaining of the spinal cords of WT EAE and *DOCK10*$^{-/-}$ EAE mice with CD3, B220, iba1, and GFAP at days (*d*) 0, 12, and 30. *C* and *D*, immunostaining of the optic nerves of WT EAE and *DOCK10*$^{-/-}$ EAE mice with CD3, B220, iba1, and GFAP at days 0, 12, and 30. Quantitative data are presented as mean values, and the *error bars* represent S.E. ($n = 3$). *, $p < 0.05$; **, $p < 0.01$; ***, $p < 0.001$, paired *t* tests. *Scale bars*, 100 μm.

in neuroinflammation and that DOCK10 could be a novel therapeutic target for MS.

Experimental procedures

Experimental animals

DOCK9$^{-/-}$, *DOCK10*$^{-/-}$, and *DOCK11*$^{-/-}$ mice were generated by homologous recombination in C57BL/6 mouse ES cells. The animals were treated in accordance with the Tokyo Metropolitan Institute of Medical Science Guidelines for the Care and Use of Animals, and all animal experiments were approved by the Institutional Animal Care and Use Committee of the Tokyo Metropolitan Institute of Medical Science. Genotyping of transgenic mice were determined by PCR using mouse tail genomic DNA and the specific primer sets (Table 1).

Histological analyses

Frozen (10 μm thick) or paraffin (7 μm thick) tissue sections of the retina, optic nerve or spinal cord were exami-

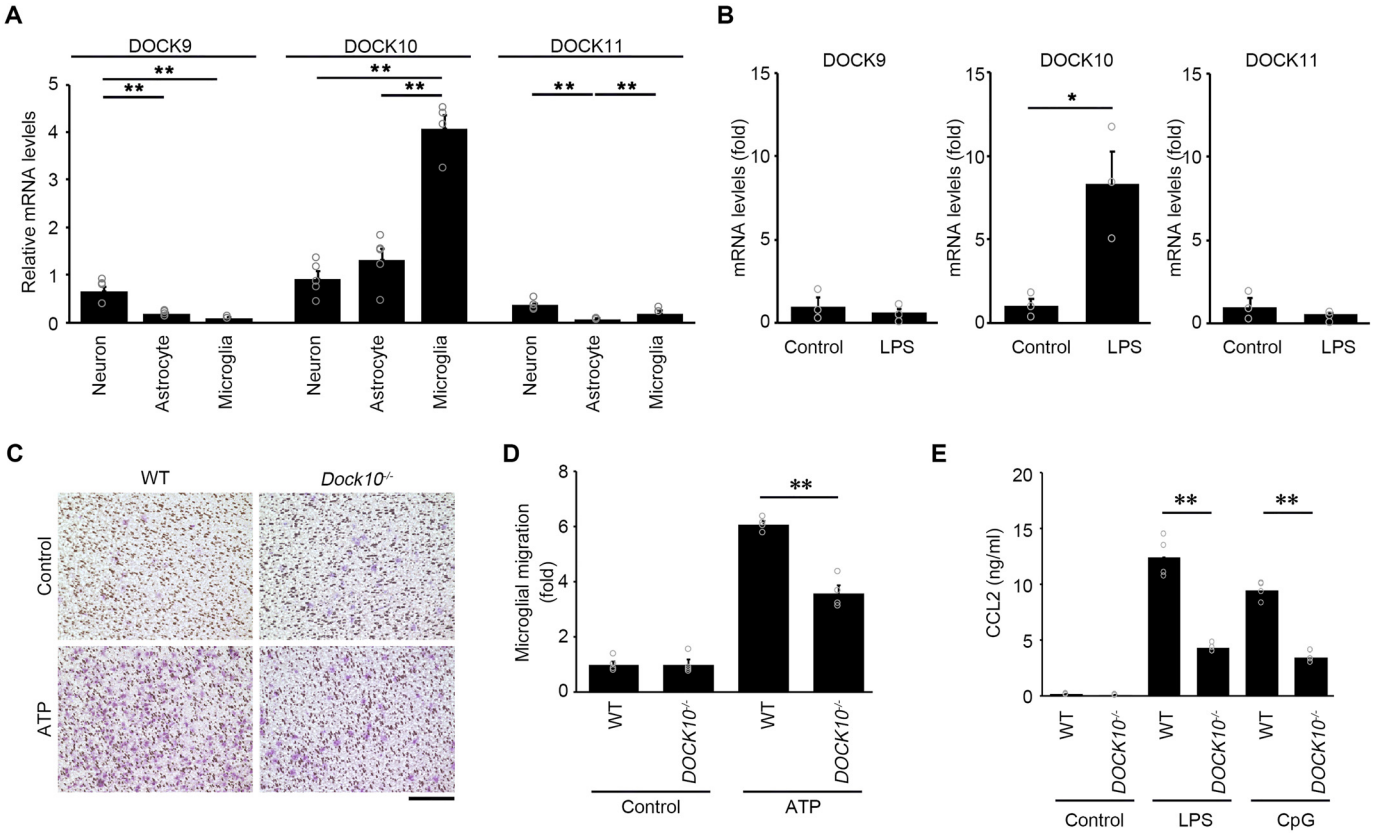

Figure 7. qPCR analysis of the DOCK-D family members in primary cultured cells and effects of *DOCK10* deficiency on activities of microglia and astrocytes. *A*, *DOCK9*, *DOCK10*, and *DOCK11* mRNA expressions were analyzed in primary cultured neurons, astrocytes, and microglial cells. The data are presented as mean values, and the *error bars* represent S.E. ($n = 4$–5). *, $p < 0.05$; **, $p < 0.01$, Tukey–Kramer test for multiple comparisons to WT. *B*, qPCR analysis of *DOCK9*, *DOCK10*, and *DOCK11* mRNA expressions in primary cultured microglial cells stimulated with LPS for 3 h. The data are presented as mean values, and the *error bars* represent S.E. ($n = 3$). *, $p < 0.05$, Student's *t* test. *C*, ATP-dependent migration of microglial cells was examined using a Boyden chamber assay. *D*, quantitative analysis of microglia migration ability in *C*. The data are presented as mean values, and the *error bars* represent S.E. ($n = 4$). **, $p < 0.01$, Student's *t* test. *E*, primary cultured astrocytes from WT and *DOCK10*$^{-/-}$ mice were stimulated with LPS or CpG for 24 h. CCL2 concentrations in the medium were measured by an ELISA. The data are presented as mean values, and the *error bars* represent S.E. ($n = 4$). **, $p < 0.01$, Student's *t* test. *Scale bar*, 100 μm.

Table 1
Sequences of primers used for genotyping PCR

Genes	Sequence (5′ → 3′)
DOCK9	
Forward 1	TTGGGAAAAGCGCCTCCCCTACCCGGTAG
Forward 2	CAGGGCTCAGGGCCACACGCAGCATTGA
Reverse 1	GTCATCTTTGTATCTCTGTCCTCGGGTCT
Reverse 2	AGCTAGGAATACAGAGGCCTGTGCCACC
DOCK10	
Forward 1	TTGGGAAAAGCGCCTCCCCTACCCGGTAG
Forward 2	GTAAGGACACTTCAAAACCAATCC
Reverse 1	GCTCTTGACTTACAAGATATATTCTAAGT
Reverse 2	CAGCCCTTGGGCTCTTTGGATATC
DOCK11	
Forward 1	TTGGGAAAAGCGCCTCCCCTACCCGGTAG
Forward 2	GGTGGCTGGAGAGATGACTTGGCAGTTAGG
Reverse 1	GCCAAATATGCTGCTGTTTGAGGTCTGAC
Reverse 2	AAATGTTATCACTCAACGGAAAACCCAGATC

ned with immunohistochemical analysis using anti-NeuN (1:1000; Merck Millipore), anti-GLAST (1:1000; Frontier Institute, Ishikari, Japan), anti-MBP (1:1000; Santa Cruz, CA), anti-CD3 (1:400; Santa Cruz), anti-B220 (1:200; Invitrogen), anti-iba1 (1:1000; Abcam, Cambridge, UK), and anti-GFAP (1:1000; Santa Cruz) antibodies. Alexa-conjugated donkey anti-goat IgG, anti-rabbit IgG, and goat anti-rat IgG (1:1000; Thermo Fisher Scientific) were used as secondary antibodies. For detection of myelin in the spinal cord and optic nerve of EAE mice, the tissues were embedded in paraffin wax, sectioned at the thickness of 7 μm, and stained with Luxol fast blue followed by hematoxylin–eosin. Stained sections were examined using a microscope (BX51; Olympus, Tokyo, Japan) connected to a DP70 camera (Olympus). The images were processed and viewed using a DP manager software (version 2.2.1.195; Olympus).

Multifocal electroretinograms

The mice were anesthetized by intraperitoneal injection of 87.5 mg/kg sodium pentobarbital. The pupils were dilated with 0.5% phenylephrine hydrochloride and 0.5% tropicamide. mfERG were recorded using a VERIS 6.0 system (Electro-Diagnostic Imaging, Redwood City, CA). The visual stimulus consisted of seven hexagonal areas scaled with eccentricity. The stimulus array was displayed on a high-resolution black and white monitor driven at a frame rate of 100 Hz. The second-order kernel, which is impaired in optic neuritis and optic neuropathy, was analyzed (34–36).

Rotarod test

Motor performance was examined by the accelerating rotarod test using a rotarod treadmill (Muromachi Kikai Co.,

Tokyo, Japan), according to the manufacturer's instructions. Briefly, the rotating speed was set to accelerate from 5 to 40 rpm over a 300-s period. Each mouse received three trials as training; then after 2-h rest, a mouse was placed on the rotating rod, and the latency to fall and speed at fall were measured.

Induction and clinical scoring of EAE

Female WT, *DOCK9*$^{-/-}$, *DOCK10*$^{-/-}$, and *DOCK11*$^{-/-}$ mice were used for the experiments. EAE was induced with the MOG_{35-55} peptide (MEVGWYRSPFSRVVHLYRNGK) at 6–8 weeks of age as previously reported (36–38). To induce EAE, a total of 200 μg of MOG_{35-55} (GenScript, Piscataway, NJ) emulsified in 200 μl of complete Freund's adjuvant (Thermo Fisher Scientific) supplemented with 4 μg/ml *Mycobacterium tuberculosis*, was injected subcutaneously into the lower flanks followed by an intraperitoneal injection of 100 ng of pertussis toxin (Thermo Fisher Scientific). Clinical signs were scored daily as follows: 0, no clinical signs; 1, loss of tail tonicity; 2, flaccid tail; 3, impairment of righting reflex; 4, partial hind limb paralysis; 5, complete hind limb paralysis; 6, partial body paralysis; 7, partial forelimb paralysis; 8, complete forelimb paralysis or moribund; and 9, death.

Flow cytometry

The cells were treated with anti-FcγRII/III (BioLegend, San Diego, CA) to block unspecific binding to Fc receptors and thereafter labeled with fluorescent antibodies for flow cytometric acquisition using a FACSCalibur flow cytometer. Data analysis was performed by the Flowjo software (Treestar, Ashland, OR). The following antibodies were used for surface staining of splenocytes: Alexa 488–conjugated anti-CD3 (1:300; BioLegend), phosphatidylethanolamine-conjugated anti-CD4 (1:1500; BioLegend), Alexa 647–conjugated anti-CD8a (1:1500; BioLegend), Alexa 647–conjugated anti-B220 (1:1000; Becton Dickinson), and phosphatidylethanolamine-conjugated anti-CD11C (1:200; eBioscience, Waltham, MA).

T-cell proliferation assay

Splenocytes were isolated and stained with 5- and 6-carboxyfluorescein diacetate succinimidyl ester (CFSE, final concentration of 0.5 μM; Dojindo, Kumamoto, Japan). 96-well ELISA plates (Iwaki, Shizuoka, Japan) were precoated with anti-CD3 antibody in PBS (2 μg/ml; Becton Dickinson) for 2 h at 37 °C. CFSE-labeled splenocytes (4×10^5) were then cultured in the anti-CD3 coated plates for 3 days at 37 °C. After culture, the cells were stained with an anti-CD4 mAb (1:1500; BioLegend) and analyzed by flow cytometry to detect CFSE dilution of gated $CD4^+$ T cells.

Chemotaxis assay

Migration assays were performed using Boyden-type 96-well plates (ChemoTx system; Neuroprobe, Gaithersburg, MD). Primary cultured microglia or bone marrow-derived macrophages (BMDMs) from *WT*, *DOCK9*$^{-/-}$, *DOCK10*$^{-/-}$, and *DOCK11*$^{-/-}$ mice were suspended in Dulbecco's modified Eagle's minimal essential medium without serum. The same medium containing CCL2 (10 ng/ml; PEPROTECH, Rocky Hill, NJ) for BMDC and ATP (50 ng/ml; BioVision, Mountain View, CA) for microglia was used to fill each well. Polycarbonate filters with 8-μm pores were placed in contact with the liquid, and the cells were dispensed over each well. The cells were seeded on polycarbonate filters and incubated at 37 °C (5% CO_2) for 3 h. The cells that had remained on the top surface of the filter were wiped with a Kimwipe, and the cells under the filter (migrated cells) were fixed with 3.7% formaldehyde for 10 min. The filter was then stained with a 0.03% crystal violet (Fujifilm, Tokyo, Japan), and individual fields were counted.

Table 2
Sequences of primers used for quantitative real-time PCR

Genes	Sequence (5′ → 3′)
DOCK9	
Forward	ACCACTTCTTGGTGGGACTG
Reverse	GTGACACATCCCTCACGTTG
DOCK10	
Forward	GATGCTGGTGGACCTTCAAT
Reverse	CACAGGGTTGGGTGTCTTCT
DOCK11	
Forward	CTGCCCAAATGAAGGAACAT
Reverse	CACATTGCAGCCTCAGAAAA
GAPDH	
Forward	TGCACCACCAACTGCTTAG
Reverse	GGATGCAGGGATGATGTTC

Quantitative real-time PCR

Quantitative real-time PCR was performed using an MyiQ single-color real-time PCR detection system (Bio-Rad) with a THUNDERBIRD SYBR qPCR mix (Toyobo, Osaka, Japan). Total RNA for PCR was prepared from tissues from WT mice and from primary cultured cells (neurons, astrocytes, and microglia) (28). Complementary DNA reverse transcribed from total RNA was amplified by using specific primers (Table 2). The data were normalized to the level of a house-keeping gene, glyceraldehyde 3-phosphate dehydrogenase mRNA.

ELISA for CCL2 measurement

Primary cultured astrocytes were treated with or without LPS (10 ng/ml) or CpG (100 nM) for 16 h. Concentrations of CCL2 in the cell culture media were determined by ELISA (R&D Systems, Minneapolis, MN).

Statistical analyses

The data are presented as mean values, and the *error bars* represent S.E. The data comparing two groups were analyzed by a two-tailed unpaired Student's *t* test. Comparison of multiple groups was performed using a Dunnett's test or Tukey–Kramer test. A value of $p < 0.05$ was regarded as statistically significant. JMP version 8.0.1 (SAS Institute, Cary, NC) was used for the statistical analyses.

Author contributions—K. N. and T. H. conceptualization; K. N., X. G., A. K., Y. A., Y. K., and C. H. data curation; K. N., Y. K., and C. H. formal analysis; K. N., X. G., and A. K. writing-original draft; A. K. and T. H. writing-review and editing; T. H. supervision.

Acknowledgments—We thank M. Kunitomo, K. Okabe, and S. Ihara for technical assistance.

References

1. Côté, J. F., and Vuori, K. (2007) GEF what?: Dock180 and related proteins help Rac to polarize cells in new ways. *Trends Cell Biol.* **17,** 383–393 CrossRef Medline
2. Laurin, M., and Côté, J. F. (2014) Insights into the biological functions of Dock family guanine nucleotide exchange factors. *Genes Dev.* **28,** 533–547 CrossRef Medline
3. Namekata, K., Kimura, A., Kawamura, K., Harada, C., and Harada, T. (2014) Dock GEFs and their therapeutic potential: neuroprotection and axon regeneration. *Prog. Retin. Eye Res.* **43,** 1–16 CrossRef Medline
4. Ruiz-Lafuente, N., Alcaraz-García, M. J., García-Serna, A. M., Sebastián-Ruiz, S., Moya-Quiles, M. R., García-Alonso, A. M., and Parrado, A. (2015) Dock10, a Cdc42 and Rac1 GEF, induces loss of elongation, filopodia, and ruffles in cervical cancer epithelial HeLa cells. *Biol. Open.* **4,** 627–635 CrossRef Medline
5. Karolak, J. A., Rydzanicz, M., Ginter-Matuszewska, B., Pitarque, J. A., Molinari, A., Bejjani, B. A., and Gajecka, M. (2015) Variant c.2262A>C in DOCK9 leads to exon skipping in keratoconus family. *Invest. Ophthalmol. Vis. Sci.* **56,** 7687–7690 CrossRef Medline
6. Hirata, E., Yukinaga, H., Kamioka, Y., Arakawa, Y., Miyamoto, S., Okada, T., Sahai, E., and Matsuda, M. (2012) *In vivo* fluorescence resonance energy transfer imaging reveals differential activation of Rho-family GTPases in glioblastoma cell invasion. *J. Cell Sci.* **125,** 858–868 CrossRef Medline
7. Abraham, S., Scarcia, M., Bagshaw, R. D., McMahon, K., Grant, G., Harvey, T., Yeo, M., Esteves, F. O. G., Thygesen, H. H., Jones, P. F., Speirs, V., Hanby, A. M., Selby, P. J., Lorger, M., Dear, T. N., *et al.* (2015) A Rac/Cdc42 exchange factor complex promotes formation of lateral filopodia and blood vessel lumen morphogenesis. *Nat. Commun.* **6,** 7286 CrossRef Medline
8. Nishikimi, A., Meller, N., Uekawa, N., Isobe, K., Schwartz, M. A., and Maruyama, M. (2005) Zizimin2: a novel, DOCK180-related Cdc42 guanine nucleotide exchange factor expressed predominantly in lymphocytes. *FEBS Lett.* **579,** 1039–1046 CrossRef Medline
9. Kang, M. G., Nuriya, M., Guo, Y., Martindale, K. D., Lee, D. Z., and Huganir, R. L. (2012) Proteomic analysis of α-amino-3-hydroxy-5-methyl-4-isoxazole propionate receptor complexes. *J. Biol. Chem.* **287,** 28632–28645 CrossRef Medline
10. Hussain, N. K., Thomas, G. M., Luo, J., and Huganir, R. L. (2015) Regulation of AMPA receptor subunit GluA1 surface expression by PAK3 phosphorylation. *Proc. Natl. Acad. Sci. U.S.A.* **112,** E5883–E5890 CrossRef Medline
11. Kuramoto, K., Negishi, M., and Katoh, H. (2009) Regulation of dendrite growth by the Cdc42 activator Zizimin1/Dock9 in hippocampal neurons. *J. Neurosci. Res.* **87,** 1794–1805 CrossRef Medline
12. Yelo, E., Bernardo, M. V., Gimeno, L., Alcaraz-García, M. J., Majado, M. J., and Parrado, A. (2008) Dock10, a novel CZH protein selectively induced by interleukin-4 in human B lymphocytes. *Mol. Immunol.* **45,** 3411–3418 CrossRef Medline
13. García-Serna, A. M., Alcaraz-García, M. J., Ruiz-Lafuente, N., Sebastián-Ruiz, S., Martínez, C. M., Moya-Quiles, M. R., Minguela, A., García-Alonso, A. M., Martín-Orozco, E., and Parrado, A. (2016) Dock10 regulates CD23 expression and sustains B-cell lymphopoiesis in secondary lymphoid tissue. *Immunobiology* **221,** 1343–1350 CrossRef Medline
14. Matsuda, T., Yanase, S., Takaoka, A., and Maruyama, M. (2015) The immunosenescence-related gene Zizimin2 is associated with early bone marrow B cell development and marginal zone B cell formation. *Immun. Ageing* **12,** 1 CrossRef Medline
15. Gerasimcik, N., He, M., Baptista, M. A. P., Severinson, E., and Westerberg, L. S. (2017) Deletion of Dock10 in B cells results in normal development but a mild deficiency upon *in vivo* and *in vitro* stimulations. *Front. Immunol.* **8,** 491 CrossRef Medline
16. Ruiz-Lafuente, N., Minguela, A., Muro, M., and Parrado, A. (2019) The role of DOCK10 in the regulation of the transcriptome and aging. *Heliyon* **5,** e01391 CrossRef Medline
17. Sakabe, I., Asai, A., Iijima, J., and Maruyama, M. (2012) Age-related guanine nucleotide exchange factor, mouse Zizimin2, induces filopodia in bone marrow-derived dendritic cells. *Immun. Ageing* **9,** 2 CrossRef Medline
18. Sakamoto, A., Matsuda, T., Kawaguchi, K., Takaoka, A., and Maruyama, M. (2017) Involvement of Zizimin2/3 in the age-related defect of peritoneal B-1a cells as a source of anti-bacterial IgM. *Int. Immunol.* **29,** 431–438 CrossRef Medline
19. Constantinescu, C. S., Farooqi, N., O'Brien, K., and Gran, B. (2011) Experimental autoimmune encephalomyelitis (EAE) as a model for multiple sclerosis (MS). *Br. J. Pharmacol.* **164,** 1079–1106 CrossRef Medline
20. Ransohoff, R. M. (2012) Animal models of multiple sclerosis: the good, the bad and the bottom line. *Nat. Neurosci.* **15,** 1074–1077 CrossRef Medline
21. Tanuma, N., Sakuma, H., Sasaki, A., and Matsumoto, Y. (2006) Chemokine expression by astrocytes plays a role in microglia/macrophage activation and subsequent neurodegeneration in secondary progressive multiple sclerosis. *Acta Neuropathol.* **112,** 195–204 CrossRef Medline
22. Mayo, L., Quintana, F. J., and Weiner, H. L. (2012) The innate immune system in demyelinating disease. *Immunol. Rev.* **248,** 170–187 CrossRef Medline
23. Mishra, M. K., and Yong, V. W. (2016) Myeloid cells: targets of medication in multiple sclerosis. *Nat. Rev. Neurol.* **12,** 539–551 CrossRef Medline
24. Bokoch, G. M. (2005) Regulation of innate immunity by Rho GTPases. *Trends Cell Biol.* **15,** 163–171 CrossRef Medline
25. Robel, S., Bardehle, S., Lepier, A., Brakebusch, C., and Götz, M. (2011) Genetic deletion of cdc42 reveals a crucial role for astrocyte recruitment to the injury site *in vitro* and *in vivo*. *J. Neurosci.* **31,** 12471–12482 CrossRef Medline
26. Alcaraz-García, M. J., Ruiz-Lafuente, N., Sebastián-Ruiz, S., Majado, M. J., González-García, C., Bernardo, M. V., Alvarez-López, M. R., and Parrado, A. (2011) Human and mouse DOCK10 splicing isoforms with alternative first coding exon usage are differentially expressed in T and B lymphocytes. *Hum. Immunol.* **72,** 531–537 CrossRef Medline
27. Xu, X., Han, L., Zhao, G., Xue, S., Gao, Y., Xiao, J., Zhang, S., Chen, P., Wu, Z. Y., Ding, J., Hu, R., Wei, B., and Wang, H. (2017) LRCH1 interferes with DOCK8-Cdc42-induced T cell migration and ameliorates experimental autoimmune encephalomyelitis. *J. Exp. Med.* **214,** 209–226 CrossRef Medline
28. Namekata, K., Guo, X., Kimura, A., Arai, N., Harada, C., and Harada, T. (2019) DOCK8 is expressed in microglia, and it regulates microglial activity during neurodegeneration in murine disease models. *J. Biol. Chem.* **294,** 13421–13433 CrossRef Medline
29. Chu, F., Shi, M., Zheng, C., Shen, D., Zhu, J., Zheng, X., and Cui, L. (2018) The roles of macrophages and microglia in multiple sclerosis and experimental autoimmune encephalomyelitis. *J. Neuroimmunol.* **318,** 1–7 CrossRef Medline
30. Kim, R. Y., Hoffman, A. S., Itoh, N., Ao, Y., Spence, R., Sofroniew, M. V., and Voskuhl, R. R. (2014) Astrocyte CCL2 sustains immune cell infiltration in chronic experimental autoimmune encephalomyelitis. *J. Neuroimmunol.* **274,** 53–61 CrossRef Medline
31. Guo, X., Harada, C., Namekata, K., Matsuzawa, A., Camps, M., Ji, H., Swinnen, D., Jorand-Lebrun, C., Muzerelle, M., Vitte, P. A., Rückle, T., Kimura, A., Kohyama, K., Matsumoto, Y., Ichijo, H., *et al.* (2010) Regulation of the severity of neuroinflammation and demyelination by TLR-ASK1-p38 pathway. *EMBO Mol. Med.* **2,** 504–515 CrossRef Medline
32. Peterson, P. K., Hu, S., Salak-Johnson, J., Molitor, T. W., and Chao, C. C. (1997) Differential production of and migratory response to beta chemokines by human microglia and astrocytes. *J. Infect. Dis.* **175,** 478–481 CrossRef Medline
33. Lee, J. W., Nam, H., and Yu, S. W. (2016) Systematic analysis of translocator protein 18 kDa (TSPO) ligands on Toll-like receptors-mediated proinflammatory responses in microglia and astrocytes. *Exp. Neurobiol.* **25,** 262–268 CrossRef Medline
34. Sutter, E. E., and Bearse, M. A., Jr. (1999) The optic nerve head component of the human ERG. *Vision Res.* **39,** 419–436 CrossRef Medline

35. Harada, T., Harada, C., Nakamura, K., Quah, H. M., Okumura, A., Namekata, K., Saeki, T., Aihara, M., Yoshida, H., Mitani, A., and Tanaka, K. (2007) The potential role of glutamate transporters in the pathogenesis of normal tension glaucoma. *J. Clin. Invest.* **117,** 1763–1770 CrossRef Medline
36. Guo, X., Harada, C., Namekata, K., Kimura, A., Mitamura, Y., Yoshida, H., Matsumoto, Y., and Harada, T. (2011) Spermidine alleviates severity of murine experimental autoimmune encephalomyelitis. *Invest. Ophthalmol. Vis. Sci.* **52,** 2696–2703 CrossRef Medline
37. Mendel, I., Kerlero de Rosbo, N., and Ben-Nun, A. (1995) A myelin oligodendrocyte glycoprotein peptide induces typical chronic experimental autoimmune encephalomyelitis in H-2b mice: fine specificity and T cell receptor V beta expression of encephalitogenic T cells. *Eur. J. Immunol.* **25,** 1951–1959 CrossRef Medline
38. Guo, X., Namekata, K., Kimura, A., Harada, C., and Harada, T. (2017) The renin-angiotensin system regulates neurodegeneration in a mouse model of optic neuritis. *Am. J. Pathol.* **187,** 2876–2885 CrossRef Medline